

(NASA-CR-197612) QUANTITATIVE  
ANALYSIS OF VOIDS IN PERCOLATING  
STRUCTURES IN TWO-DIMENSIONAL  
N-BODY SIMULATIONS (Kansas Univ.)  
12 p

N95-18949

Unclass

G3/77 0038404

**Quantitative Analysis of Voids in  
Percolating Structures in  
Two-Dimensional N-Body Simulations**

**Patrick M. Harrington, Adrian L. Melott,  
and**

**Sergei F. Shandarin**

Department of Physics and Astronomy  
University of Kansas, Lawrence, Kansas 66045

THE UNIVERSITY OF KANSAS

---

Department of Physics and Astronomy

Lawrence, Kansas 66045

---

**Quantitative Analysis of Voids in  
Percolating Structures in  
Two-Dimensional N-Body Simulations**

**Patrick M. Harrington, Adrian L. Melott,  
and  
Sergei F. Shandarin**  
Department of Physics and Astronomy  
University of Kansas, Lawrence, Kansas 66045

**Quantitative Analysis of Voids in  
Percolating Structures in  
Two-Dimensional N-Body Simulations**

**Patrick M. Harrington, Adrian L. Melott,  
and  
Sergei F. Shandarin**  
Department of Physics and Astronomy  
University of Kansas, Lawrence, Kansas 66045

# Quantitative Analysis of Voids in Percolating Structures in Two-Dimensional N-Body Simulations

Patrick M. Harrington, Adrian L. Melott, and Sergei F. Shandarin

*Department of Physics and Astronomy, University of Kansas, Lawrence, KS 66045*

## Abstract

We present in this paper a quantitative method for defining void size in large-scale structure based on percolation threshold density. Beginning with two-dimensional gravitational clustering simulations smoothed to the threshold of nonlinearity, we perform percolation analysis to determine the large scale structure. The resulting objective definition of voids has a natural scaling property, is topologically interesting, and can be applied immediately to redshift surveys.

## I. INTRODUCTION

There has been increasing interest in large voids in the galaxy distribution. However, in large-scale theory and practice, there currently exist many different definitions of a void (for discussion see Sahni, Sathyaprakash & Shandarin, 1993). Our purpose here is to present an objective and quantitative method for defining voids. We use an algorithm developed by Kauffmann (see Kauffmann & Melott 1992, hereafter KM) to locate voids. We use a percolation technique suggested by Shandarin (1983) in the form developed by Klypin & Shandarin (1993, hereafter KS) to determine the threshold density. We perform the analysis on two-dimensional N-body generated density distributions used in the work of Beacom et al (1991, hereafter BDMPS).

The choice of the percolation threshold is motivated by the fact that it marks a change of topology. In the absence of percolation, the regions above the density threshold are isolated. On the contrary, in two-dimensional (hereafter 2-D) space, if the fraction above the threshold percolates, the fraction below the threshold forms isolated voids.

We perform this work in two dimensions because coding and de-bugging are obviously simpler and visualization is easier. The agreement between the 2-D work of BDMPS and Melott & Shandarin's 3-D work (1993, hereafter MS) is very impressive, suggesting 2-D is a good guide to what will happen in 3-D. The technique can be easily applied to two-dimensional galaxy samples, as well as to the microwave temperature fluctuation maps. After testing this method in 2-D we plan to study more realistic 3-D distributions.

## II. NUMERICAL SIMULATIONS

The numerical models are the ones used in the work of BDMPS. They are  $512^2$  density arrays that simulate various epochs of gravitational clustering. The models are evolved with a particle-mesh code by solving Poisson's equation and are equivalent to a cross-section of a three-dimensional  $\Omega = 1$  FRW universe with two-dimensional density perturbations. Thus, they exhibit a subset of the behavior possible in three dimensions. The initial conditions for these models are pure power-law spectra with  $n = 2$ ,  $n = 0$  and  $n = -2$ , and are analogous to  $n = 1$ ,  $n = -1$  and  $n = -3$ , respectively, in three dimensions. For more detailed information see BDMPS. The  $n = -2$  model is analogous to the CDM model on small scales, and the  $n = 0$  model is analogous to the part of the CDM spectrum reaching non-linearity at  $z \sim 0$ . The  $n = 2$  spectrum is analogous to that part of the spectrum coming within the horizon at any moment in most inflationary theories of the generation of perturbations. For each type of initial condition we evolve density arrays representing progressive epochs by introducing a non-linearity frequency  $k_{NL}$ , which corresponds to the transition into non-linear evolution.  $k_{NL}$  is defined by:

$$D^2(t) \int_0^{k_{NL}} P(k) d^2k = 1,$$

where  $D(t)$  is the growing mode of gravitational instability,  $D(t) = a(t)$  for the  $\Omega = 1$  universe,  $a(t)$  is the cosmological scale factor and, in the absence of pressure and radiation terms,  $a(t) \propto t^{2/3}$ . The non-linearity frequency is chosen to be  $k_{NL} = 2^r k_f$  where  $r = 2, 3, \dots, 7$  and  $k_f = 2\pi/L$  where  $L$  is the size of the simulation box (512 grid units). The Nyquist frequency for these simulations is  $k_N = 256k_f$ . Additionally, we have run four realizations of each model at each epoch in order to average our results. We have, therefore, four realizations for each of six epochs in both the  $n = 2$  and  $n = 0$  simulations and for each of five epochs in the  $n = -2$ . We also decided to study a pure Gaussian distribution for the  $n = 2$  and  $n = 0$  models. For both models we ran ten realizations of a Gaussian distribution. Thus we have a total of eighty-eight files studied, averaged into nineteen sets of results.

## III. SMOOTHING

We smooth each density distribution by Fourier convolution with the Gaussian window

$$W(R) = e^{-R^2/2R_S^2}.$$

We specify the smoothing length for each distribution as  $R_S = R_1$  where  $R_1$  is the value for which the RMS density fluctuation  $\delta\rho/\rho = 1$ . As reported in BDMPS,  $R_1 = 0.8k_{NL}^{-1}$  is extremely stable and is more reliable than smoothing with the correlation length. Another advantage of this choice is that  $R_1$  in our universe is about  $8h^{-1}Mpc$ , close to the mean galaxy separation. Thus the smoothing will remove most noise due to discreteness effects, and may somewhat lessen the difference between the coordinate and redshift spaces.

## IV. PERCOLATION

Percolation theory has been a tool available to physicists for some time. It is used mainly to study phase transitions such as the spontaneous alignment of spin occurring at the Curie temperature. Zel'dovich (1982) and Shandarin (1983) were the first to apply percolation to cosmology, using it as a tool to study topological properties of non-linear density fields.

In essence, we use percolation to study phase transitions also. In our case however, it is not the system under study that is evolving, we have already evolved our simulations to the various points in time or epochs we wish to study. Rather, we take each of our 'snap shots' of gravitational clustering and allow the 'threshold density' to change. We choose an initial threshold density and increment or decrement this density until percolation in the over-dense or under-dense phase is reached using a square-lattice percolation algorithm. The percolation threshold is the point at which the transition is made from discontinuous clusters to a global cluster which spans the simulation box. The density at which this threshold is reached is called the percolation density. This percolation density is applied to the smoothed density files such that anything equal to or above percolation density becomes a 1 and anything below becomes a 0. We call this our percolated file. For the sake of simplicity, we will call regions above the threshold 'superclusters' and those below it 'voids.' We wish to stress that these are not necessarily identical to the observationally based use of these words, and emphasize this by using single quotes.

In the ideal continuous 2-D world, percolation in the over-dense phase would mean the absence of percolation in the under-dense phase and vice-versa. However, we study percolation on a 2-D square lattice, and therefore it may be possible that neither phase percolates. In order to make the procedure symmetric, we apply the void search at the percolation threshold in the over-dense phase and, measuring the 'supercluster' sizes, we use the percolation threshold in the under-dense phase. This technique can be used to study the largest voids when they are isolated, since the over-dense phase percolates and vice-versa. One can find a more detailed discussion of percolation in 2-D systems in Dominik and Shandarin (1992).

## V. VOID SEARCH

We perform a 'void' search on the percolated file. The 'void' search algorithm (KM) first finds the largest square of empty cells in the percolated file. Any empty cells along its four sides are then added to this base 'void', subject to the criterion that the length of the fill-in cannot be less than two-thirds the base 'void' length. When the fill-in is complete, the next largest square is found and cells are added to it. This process continues for smaller and smaller squares until all the 'voids' in a particular simulation are found. We weight each 'void' size by its predominance in the simulation. We characterize each simulation by the diameter of a circle of area equal to the weighted average 'void' size.

$$\langle D \rangle = \frac{\sum d W_d}{\sum W_d}$$

where the summations are over the range of 'void' sizes,  $d = 2, 3, \dots, d_{MAX}$  and

$$W_d = \frac{N_d d^2}{d_{MAX}^2}$$

is the weight of 'voids' of size  $d$ .  $N_d$  is the number of 'voids' of size  $d$ . For purposes of comparison we performed a 'supercluster' search by percolating along under-dense regions so that the 'void' search was actually finding the typical sizes of the 'superclusters.'

## VI. RESULTS AND DISCUSSION

We present the results in the form of the percentage area occupied by 'voids' or 'superclusters' as a function of the diameter in figures 1-3, for  $n = 2, 0, -2$  respectively. Panel (a)

in figure 1 and 2 shows the distribution for the Gaussian fields with the corresponding power spectra. One can see that in Gaussian fields there is no statistical difference between the 'void' and 'supercluster' distributions, which was of course anticipated. It is worth stressing that the total area in 'voids' and 'superclusters' is only  $\approx 12\%$  in the  $n = 2$  model and  $\approx 31\%$  in the  $n = 0$  model. It reflects the fact that the 'void' search algorithm can measure only large 'voids' (see figure 4). One can see also that in the range  $D \sim 0.005$ , there are about 2.5 times more 'voids' in the  $n = 0$  model than in the  $n = 2$  model and there are a few larger 'voids' as well. Both features are in agreement with the greater smoothness of the  $n = 0$  model.

The non-linear stages shown in panels b through g of figure 1 and 2 show the major difference between the  $n = 2$  and  $n = 0$  models: in the  $n = 2$  model 'superclusters' occupy more area than 'voids' and the largest structures are also 'superclusters,' in the  $n = 0$  model the opposite is true. The degenerate  $n = -2$  model demonstrates that 'voids' are always the dominant structures.

The  $n = 2$  model shows that both the 'voids' and 'superclusters' roughly scale with the scale of non-linearity  $\lambda_{NL}$ , and the  $n = -2$  model does not, as can be seen in figure 1 through 3 and especially in figure 5. The mean diameter of 'superclusters' is slightly but significantly greater than that of 'voids' in the  $n = 2$  model, and both are about 2 times smaller than  $\lambda_{NL}$ , shown as a dotted line in figure 5.

In the  $n = 0$  model 'voids' are a little larger than 'superclusters' and the difference with  $\lambda_{NL}$  is somewhat less, about 1.8 times. The models also do not display quite as good scaling with  $\lambda_{NL}$  as the  $n = 2$  model.

As previously mentioned in the section on the void search routine, we don't necessarily include all of the area below the percolation threshold in 'voids.' The 'void' search routine was written to approximate circular 'voids.' This is most obvious in figure 4, where the early epochs show a combined 'void'/cluster area of considerably less than 100%. In the later epochs, the 'voids' become larger and more circular; less 'void' area is lost due to the two-thirds requirement during fill-in (see description of void search). The careful observer will also notice that a few of the data points are slightly above 100%, most noticeably the last two data points on the  $n = -2$  (dashed) line. This is simply because we measure 'voids' at the percolation threshold of the over-dense regions and 'superclusters' at that of the under-dense regions, and these percolation thresholds are not identical.

The advantages of our approach are both theoretical and practical. The smoothing we use removes discreteness effects and our choice of smoothing length is insensitive to statistical fluctuations. The use of percolation objectively defines a connected structure, and its combination with an objective measure of void size remedies its major shortcoming as a large-scale structure statistic, i.e., it does not give rise to a physical lengthscale associated with percolating structures. As shown in earlier work, the results of percolation studies can be connected with the initial conditions that generated the structures.

## VII. ACKNOWLEDGMENTS

We are grateful for financial support from the University of Kansas GRF fund, NASA Grant NAGW-2923, and NSF Grants AST-9021414 and OSR-9255223. PMH is especially grateful for support from the NSF Research Expenses for Undergraduates program. Our computer simulations were done on a grant of Cray-2 time at the National Center for Supercomputing Applications. We wish to thank Guinevere Kauffmann for use of and advice on her void search software.

## VIII. REFERENCES

- Beacom, J.F., Dominik, K.G., Melott, A.L., Perkins, S.F., & Shandarin, S.F. 1991, *ApJ*, 372, 351  
 Dominik, K.G., & Shandarin, S.F. 1992, *ApJ*, 393, 450  
 Kauffmann, G., & Melott, A.L. 1992, *ApJ*, 393, 415  
 Klypin, A.A., & Shandarin, S.F. 1993, *ApJ*, 413, 48  
 Melott, A.L., & Shandarin, S.F. 1993, *ApJ*, 410, 469  
 Sahni, V., Sathyaprakash, B., & Shandarin, S.F. 1993, in preparation  
 Shandarin, S.F. 1983, *Sov. Astron. Lett.*, 9, 104  
 Zel'dovich, Ya.B. 1982, *Sov. Astron. Lett.*, 8, 102

## IX. FIGURE CAPTIONS

Figure 1a) Percentage area occupied by 'voids' (solid lines) and 'superclusters' (dashed lines) of size  $L$  (units of box size) for a purely Gaussian density distribution with  $k_c = 256k_f$  in the  $n = 2$  model.

Figure 1b) Percentage area occupied by 'voids' (solid lines) and 'superclusters' (dashed lines) of size  $L$  (units of box size) for the epoch  $k_{NL} = 128$  in the  $n = 2$  model.

Figure 1c to 1h) Same as Fig. 1b but  $k_{NL}$  as specified on plot.

Figure 2) Same as Fig. 1 for  $n = 0$  model

Figure 3a) Same as Fig. 1 for  $n = -2$  model except that only stages  $k_{NL} = 64, 32, 16, 8, \text{ and } 4$  are shown.

Figure 4) Sum of areas occupied by both 'voids' and 'superclusters' versus  $\lambda_{NL}$  for  $n = 2$  (solid line),  $n = 0$  (dotted line) and  $n = -2$  (dashed line) models.

Figure 5a) Evolution of mean 'void' size (solid line) and 'supercluster' size (dashed line) versus  $\lambda_{NL}$  in the  $n = 2$  model.  $d = \lambda_{NL}$  (dotted line) is included for comparison.

Figure 5b) Same as Fig. 5a but in the  $n = 0$  model.

Figure 5c) Same as Fig. 5a but in the  $n = -2$  model.



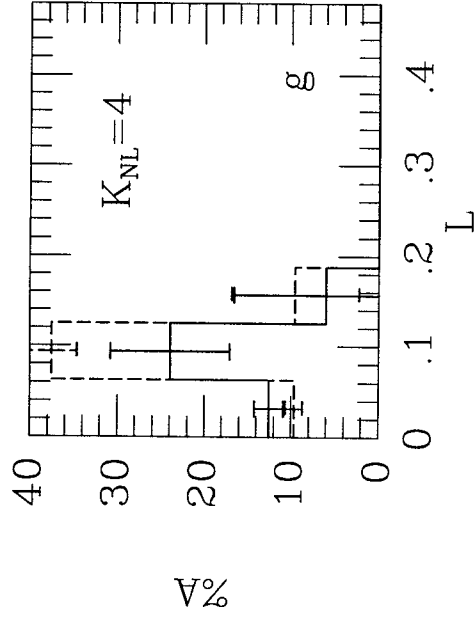
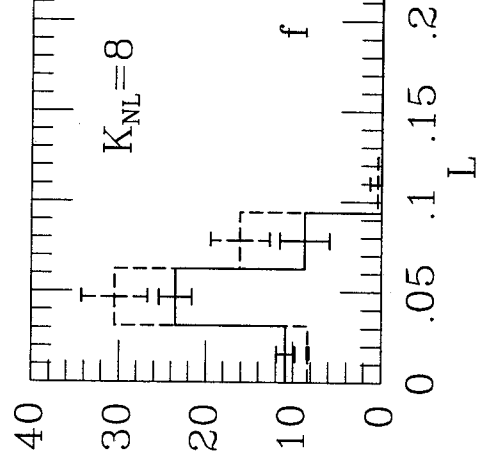
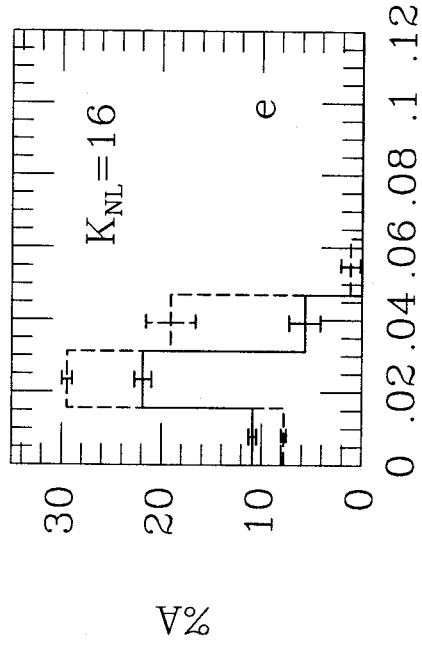
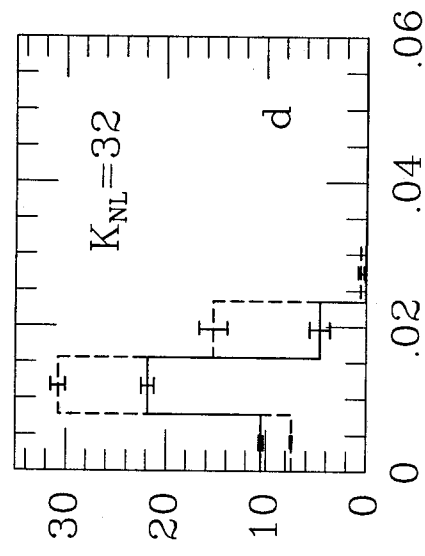
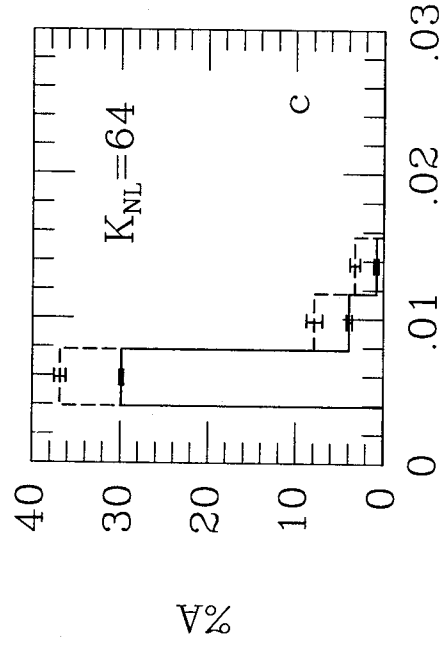
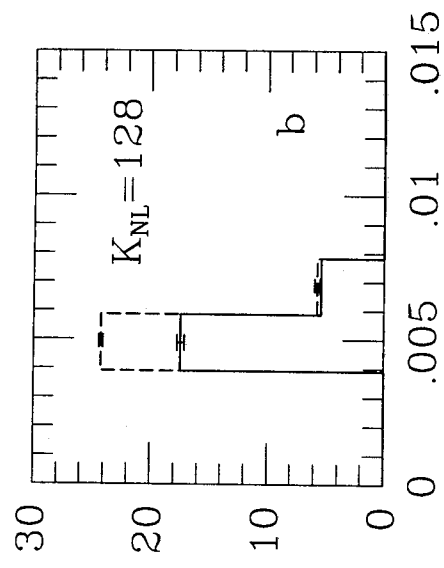
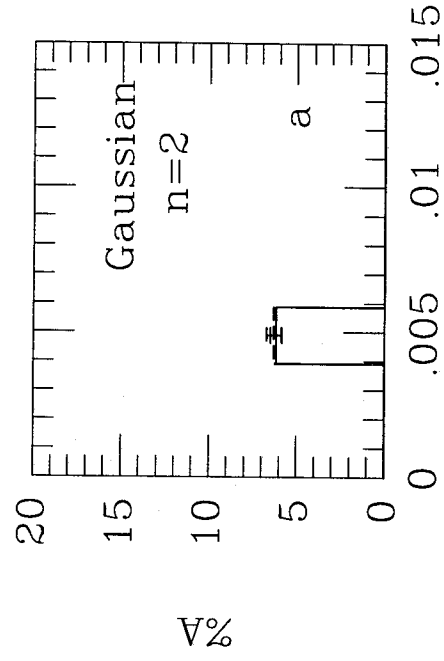


Fig. 1

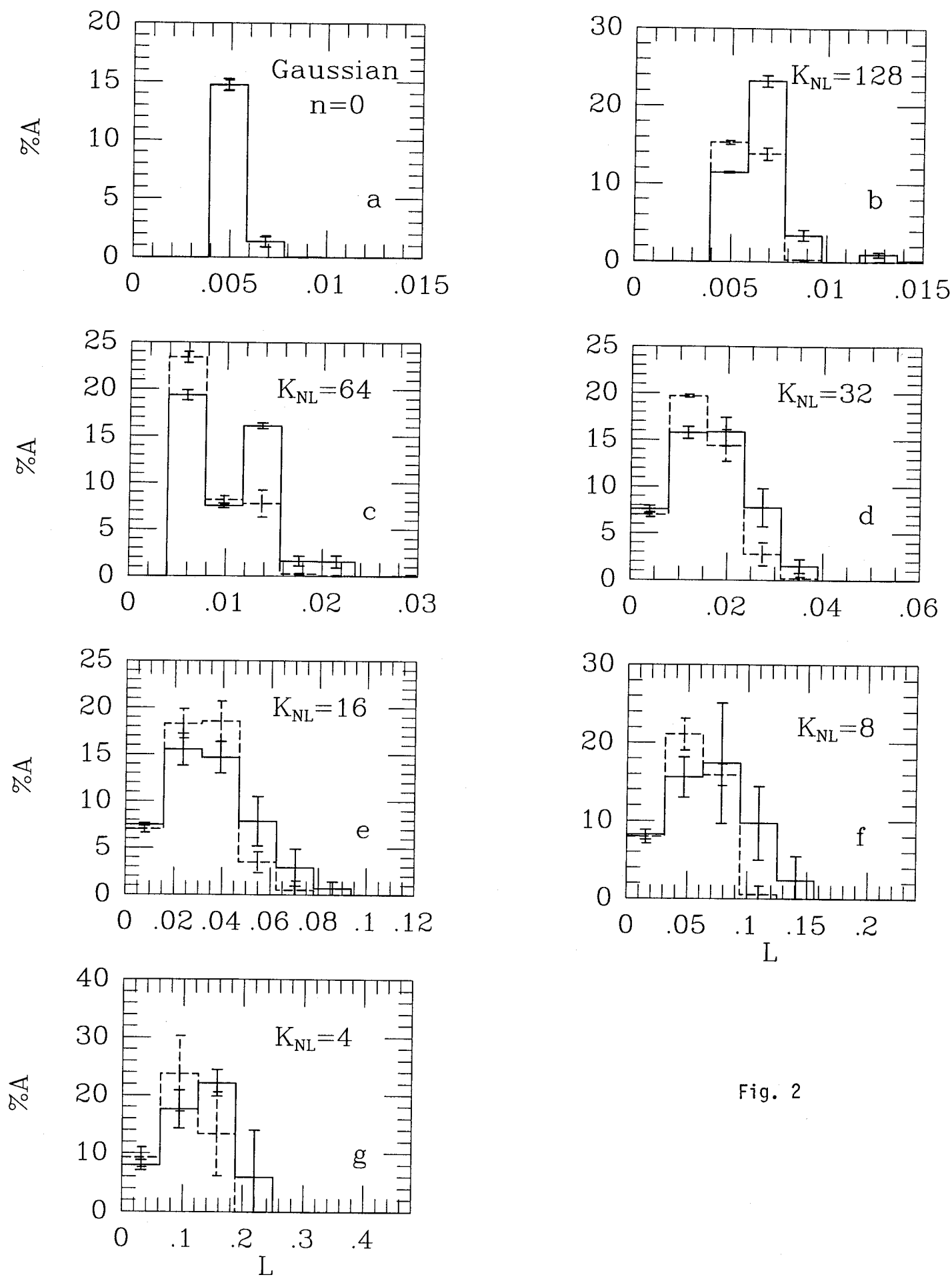


Fig. 2

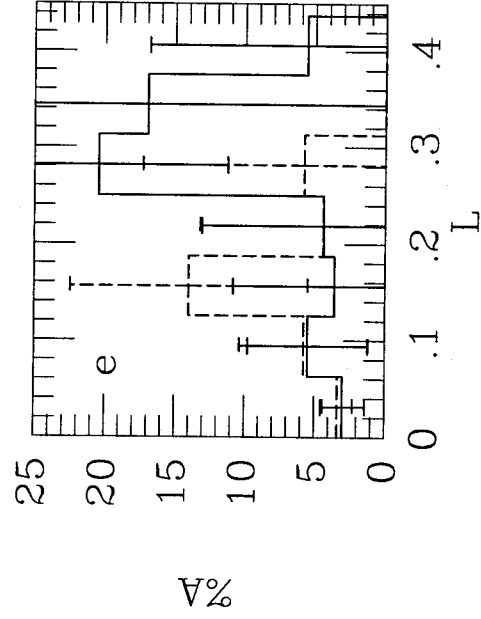
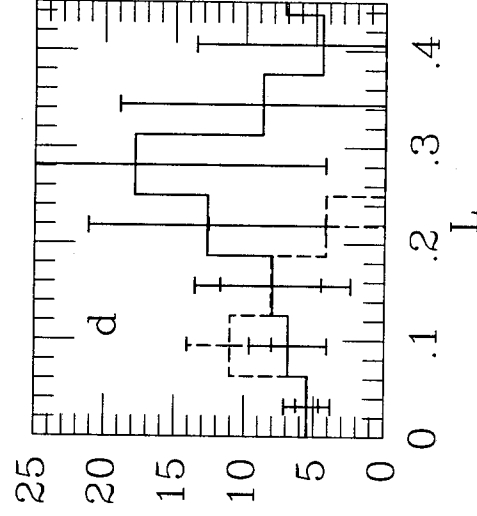
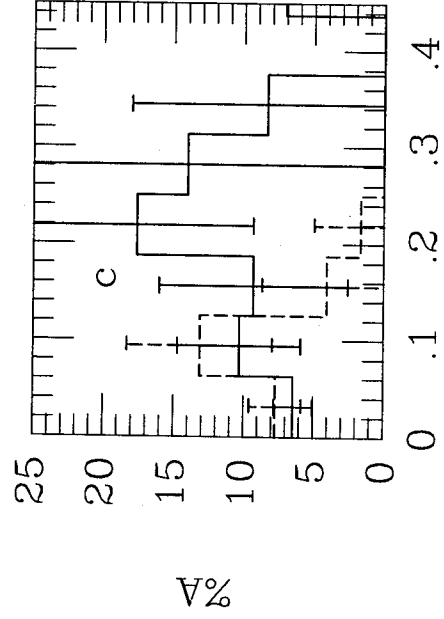
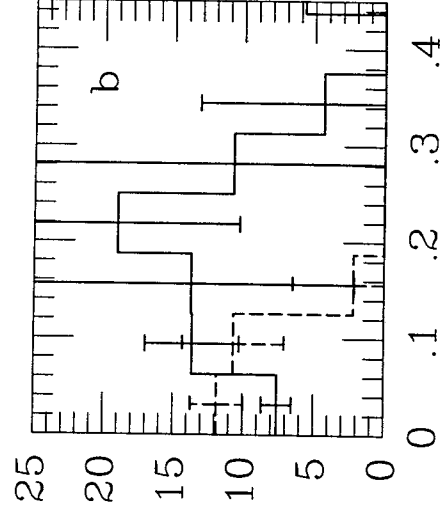
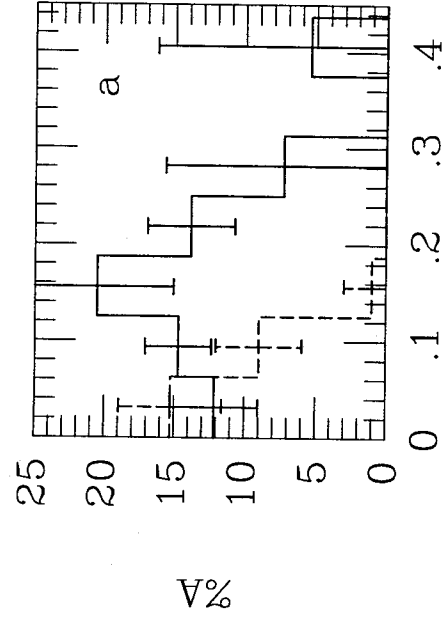


Fig. 3

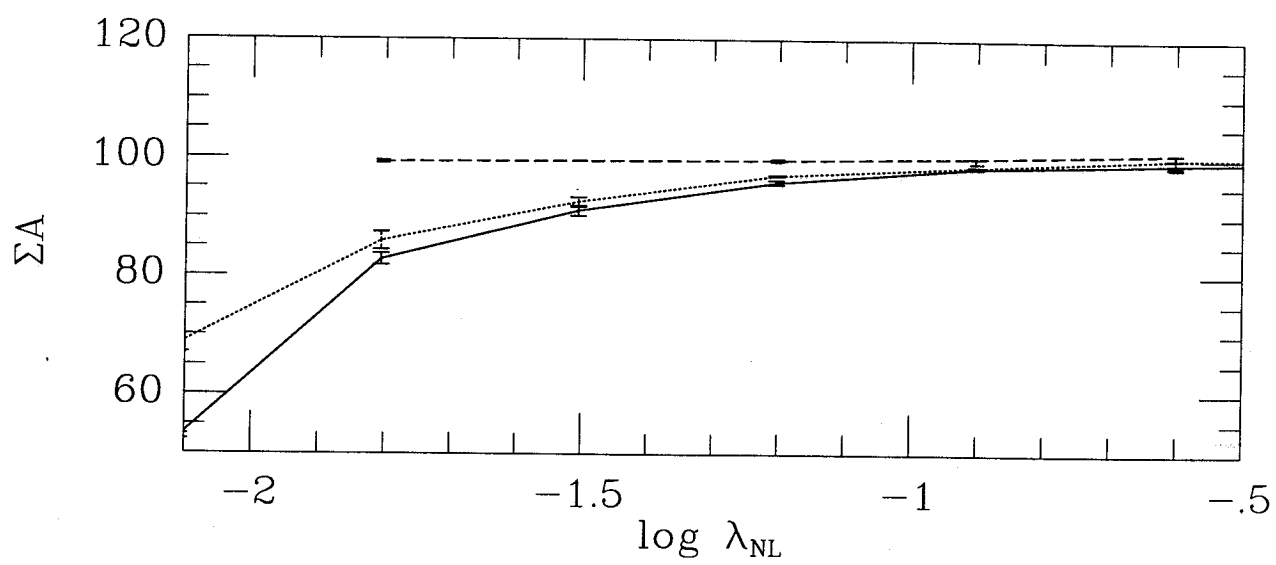


Fig. 4

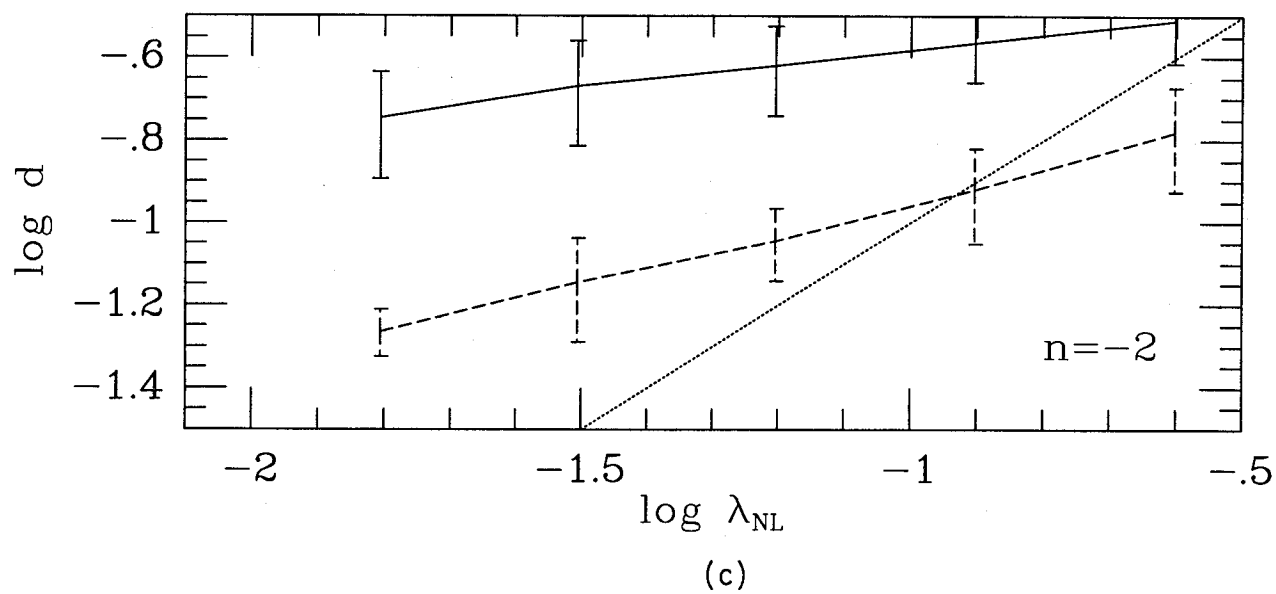
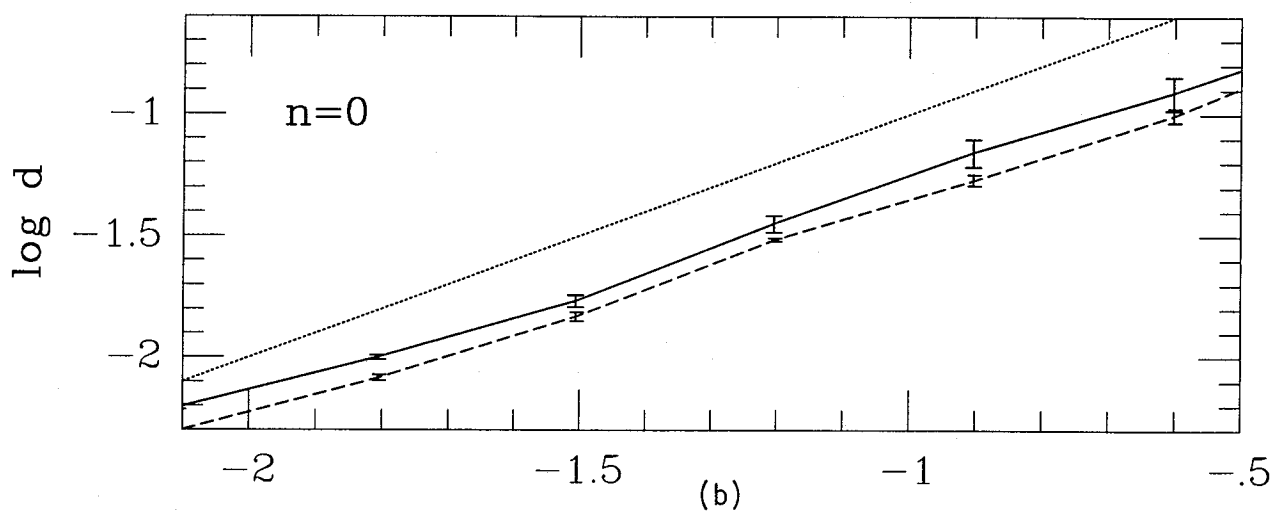
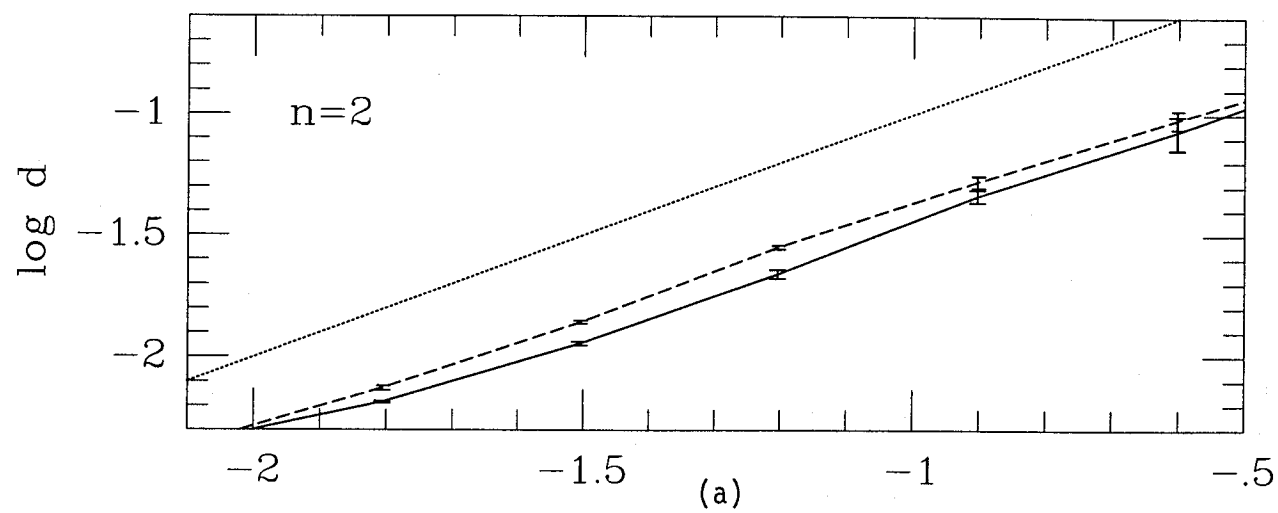


Fig. 5